Physica E 41 (2008) 292–298

Contents lists available at ScienceDirect

Physica E

journal homepage: www.elsevier.com/locate/physe

Blue and yellow luminescence of GaN nanocrystals-doped SiO_2 matrix

M. Bouguerra [a,*], M.A. Belkhir [a], D. Chateigner [d], M. Samah [a], L. Gerbous [b], G. Nouet [c]

[a] Laboratoire de Physique Théorique (LPT), Département de Physique, Université de Bejaia, Bejaia 06000, Algeria
[b] Centre de Recherche Nucléaire d'Alger (CRNA), 02 Bd de Frantz Fanon BP 399, Alger, Algeria
[c] SIFCOM-ENSICAEN 6 Bld Maréchal Juin, Caen 14050, France
[d] CRIS-MAT.ENSICAEN, Université de Caen Basse-Normandie, 6 Bld Maréchal Juin, Caen 14050, France

ARTICLE INFO

Article history:
Received 29 April 2008
Received in revised form
14 July 2008
Accepted 15 July 2008
Available online 19 September 2008

PACS:
79.60.Jv

Keywords:
GaN nanocrystal
Yellow luminescence
Blue luminescence
PLE
PL

ABSTRACT

GaN–SiO_2 nanocomposite and GaN-free nanopowder are studied. X-ray diffraction (XRD), transmission electron microscopy (TEM), photoluminescence (PL) and photoluminescence electron excitation (PLE) techniques are used to investigate their structural and optical properties. Microstructural study reveals flattened sphere-like crystallites with a mean size of around 150 nm in the GaN–SiO_2 sample, and multimodal size distributions in the raw GaN powder. A strong yellow and blue luminescence centred at ~2.25 and ~2.9 eV, respectively, is observed in the room-temperature PL spectra of the nanocomposite with the one of the powder. Ambient PLE measurements reveal several zero-phonon lines of the YL line, which lead to several type defects. The optical measurements are correlated with structural defects such as $(V_{Ga}–O_N)^{2-}$, $(V_{Ga}–O_{2N})^{1-}$ and surface defects.

1. Introduction

Nanocrystals have stimulated great interest due to their importance in basic scientific research and potential technological applications. These materials exhibit unique chemical and physical properties, differing substantially from those of the corresponding bulk solids because of their small size and extremely large surface-to-volume ratio. It is well known that this new category of materials offers a number of valuable advantages, like tuning the gap with size or weak temperature dependence of the nanocrystal optoelectronic characteristics. For blue-UV light-emitting diodes (LEDs) and laser diodes (LDs), wide band gaps and high chemical stability are required, which is similar to GaN and ZnO crystals.

The III-nitrides such as AlN, GaN and InN or ternary alloys are very promising materials for their use in high-power, high-temperature electronic devices such as UV detectors, waveguides, Bragg reflectors or blue-UV LDs and LEDs [1,2]. Earlier studies revealed that GaN-based LEDs achieve high brightness in blue and green spectral ranges with viable operating lifetime in spite of the high density of dislocations (~10^{10} dislocations/cm^2) [3]. However, six orders of magnitude fewer dislocations are sufficient to completely annihilate comparable conventional GaAs-based laser capabilities [4]. Ponce and Bour [5] suggest that the localisation of defects at the grain boundary is accounted for lasing observed in GaN. Nowadays, it is established that the recombination in the active layer of InN in LDs is enhanced by self-formed quantum-dot (QD)-like structure or by localisation of the excitons by potential fluctuations induced by the segregation of In at the growth stage [6,7]. This information engendered enlargement of the interest in GaN nanocrystals.

In general, the undoped GaN nanocrystals' luminescence is dominated by the so-called yellow (YL) and blue (BL) at 2.2 and 2.9 eV, respectively. The YL line is a broad luminescence and universal feature in n-type GaN. This band is attributed to electron transition from the conduction band or/and shallow donor to deep acceptor levels located approximately at 0.8 eV above the valence band, but the microscopic acceptor nature remains controversial. Today the prevailing view is that V_{Ga} and complex, particularly $V_{Ga}–O_N$, are mainly responsible for YL [8]. BL-related defects are also not firmly attributed. Such luminescence is observed in undoped GaN and in C- and Zn-doped GaN. Widmann et al. [9] attributed the luminescence of wurtzite GaN QDs, located at 2.9 eV, to piezoelectric field engendered by interface deformations. Recently, Shim et al. [10] and Shimada et al. [11] attributed the BL to amorphous GaN (a-GaN), while Li et al. [12] have shown

* Corresponding author.
E-mail address: bouguerradjitou@yahoo.fr (M. Bouguerra).

1386-9477/$ - see front matter © 2008 Elsevier B.V. All rights reserved.
doi:10.1016/j.physe.2008.07.010

that the BL of the undoped GaN is closely related to crystalline quality, i.e., the existence of grain boundaries and other native structural defects. Assuming this hypothesis, we expect a large contribution of the BL to the luminescence spectra of GaN nanocrystals, since the large surface of the nanocrystallites can be treated strictly as a structural defect or grain boundary. On the other hand, Reshchikov et al. [13] have demonstrated that the BL of the undoped GaN is hardly related to the surface state and can be enhanced or quenched by the appropriate chemicals and/or thermal treatments.

In the present paper, we investigate the structural and optical characteristics of GaN-free powder and GaN–SiO_2 nanocomposite. We report the YL and enhanced BL of GaN nanocrystals dispersed in SiO_2 amorphous matrix elaborated using a sol–gel method. We combined the photoluminescence (PL) and photoluminescence excitation (PLE) measurements to confirm that YL is related to V_{Ga}–O_N complex defects and connect the BL to the surface state defects. X-ray diffraction (XRD) and transmission electron microscopy (TEM) analyses are used in order to measure the nanocrystals' sizes.

2. Experiments

The elaboration method used in this work is the same as the one described by Duval et al. [14] with some modifications. Tetraethoxysilane, water and ethanol were mixed in the following quantities: 21.4, 2.25 and 13.6 ml, respectively. Then, the solution was catalysed by traces of HCl (~5 μl). The mixture was stirred for 24 h at ambient temperature (32 °C) to achieve complete hydrolysis. Another solution was obtained by mixing 70 ml of acetone, 4.5 ml of deionised water and 0.2 ml of ammonium hydroxide and stirred for several minutes.

The two solutions were then shaken and jiggled. Before gelification, a-GaN fine powder was added to this final solution and also shaken for homogenization. The solution was left for some hours to let the biggest GaN particles precipitate. Then, the colourless solution above was used to obtain the GaN–SiO_2 samples.

The obtained xerogels were stored at 32 °C during 10 weeks. Such a long storage step is necessary to avoid gallium oxide formation and diffusion of the matrix elements inside the crystals, and, on the other hand, to ensure the residual sol evacuation out off the samples.

We characterised both the raw GaN powder and the GaN–SiO_2 composite using TEM, HRTEM, XRD, PL and PLE measurements. XRD measurements were operated in reflection geometry, using a curved position sensitive detector (CPS 120 from INEL) and the CuKα monochromatised radiation [15]. An incidence angle of 10° ensured an irradiated surface of several mm^2 on the sample. We used an acquisition time of 3 h, meaning each point in the 10–90° the range 2θ is measured for 3 h. Using such a counting statistics, we aimed at revealing any crystallites potentially remaining in the sample after the sol–gel process, which would be present above 1‰ of the total volume. This volume resolution threshold is, however, decreased for small-sized crystallites, particularly when embedded in the amorphous matrix, as it is the case for our samples.

XRD diagrams were fitted using Rietveld refinement within the MAUD package [16], in order to extract the volumic ratio of crystallites and silica. The amorphous silica was fitted using the Le Bail approach [17], while the crystallite shapes were refined in the Popa anisotropic model [18]. An arbitrary texture correction [19] was used to compensate for eventual small structure changes.

In addition, PL and PLE spectra are measured. PL and PLE measurements were performed on a Hitashi 850 fluorescence spectrometer at room temperature. The excitation wavelength was produced by a xenon lamp equipped with a grating monochromator.

3. Results and discussion

The XRD diagram for the GaN–SiO_2 composite (Fig. 1) exhibits the GaN peaks superposed to large modulations due to the silica glass matrix. We used the cristobalite cubic polymorph of silica to simulate the amorphous matrix. The refinement provided a cristobalite cell parameter of 6.760(6) Å, an isotropic mean crystallite size of 13.5(2) Å and isotropic crystallite microstrains of 0.122(3) rms. The mean crystallite size indicates the amorphous character of the silica with a loss of coherence after around two unit cells on average.

GaN particles crystallize in the wurtzite structure with refined lattice parameters of $a = 3.1878(2)$ Å and $c = 5.1825(4)$ Å. These are close to the bulk values (Crystallography Open Database [20] no. 9008868). No peak shift is observed compared to the bulk values as expected for an inert amorphous matrix which does not induce stress on the GaN crystallites. The incorporated volume of GaN in the matrix is refined to 1.2(3)%. The anisotropic mean shape of the crystallites is a flattened sphere with a mean diameter of 153 nm, a short axis along $[0\,0\,\ell]$ of 145(2) nm and a long transverse direction in the (a, b) plane of 166(3) nm (inset in Fig. 1). These values were refined using two free parameters for the Popa harmonic series. No significant improvement of the fit was noticed for a larger number of free harmonic coefficients. The crystallites' microstrains did not show an anisotropic character, with a mean distortion of 0.001(3) rms. These are not large microstrain values but are, however, one order of magnitude larger than in typically well-crystallised powders and could participate in enhancing surface effects.

Fig. 2 (a–h) shows TEM images of the GaN powder. We observe a multimodal distribution of particle sizes and shapes (Fig. 2a and b). Little platelet-like-shaped crystallites are visible, together with biggest spherical-like ones. The average of such shapes is coherent with the mean objects determined by XRD. A large number of grains seen by TEM exhibit sizes of several hundred nanometres, i.e. a typical size much larger than that determined by XRD, which could appear to contradict each other's approach. However, one has to realise that using XRD all the contributions from large and small crystals are convoluted and seen as mean sizes. The presence of small and large grains in TEM images is then not out of the XRD mean size. Furthermore, the TEM micrographs (Fig. 2b) reveal that the large grains are in fact aggregation of smaller ones that could be the coherent domains (crystallites) seen by XRD. The average crystallite sizes determined by the two approaches are then in good agreement. The most interesting feature appears in the grain surface's details, where we see agglomeration of small crystallites (with a typical size smaller than 50 nm) around the big conglomerates (Fig. 2d and e). Thus, we could expect large and singular optical contribution from the atoms located at the GaN–SiO_2 interfaces.

The room-temperature PL spectra from the GaN-free powder at 325 and 360 nm wavelength excitations (Fig. 3) exhibit a similar behaviour below 2.60 eV, with a broad band peaking at 2.255 eV. However, significant differences can be observed above this value. On the PL measurement at $\lambda_{ex} = 325$ nm (Fig. 3b, line), we see an enhanced BL contribution in the 2.8–2.9 eV range. The PL spectra, for the 325 and 360 nm excitations, exhibit three weak emission peaks in this range, located at 2.92, 3.02, 3.28 eV and 2.85, 3.02, 3.23 eV, respectively. The UV luminescence (UVL) is attributed to donor–acceptor pair transitions involving deep donors or e–A transitions. In bulk GaN, unlike the yellow line, which remains

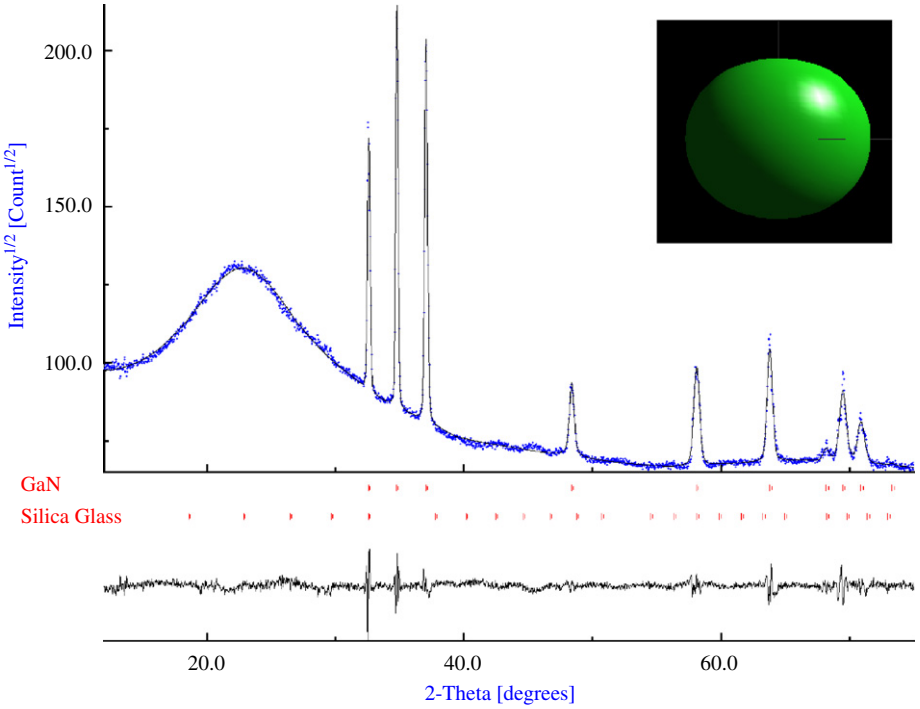

Fig. 1. XRD diagram showing the experimental (blue points) and fit (line) of the GaN–SiO_2 composite. GaN and silica peak positions are shown, together with the difference curve between simulation and experiment. Note the large bump of silica glass correctly reproduced from the Le Bail model. This fit was obtained with the following reliability factors: $R_w = 3.31\%$, $R_{exp} = 1.11\%$, GoF = 8.9. Inset: illustration of the mean crystallite shape.

nearly unchanged with temperature variations up to room temperature, the UVL quenches at temperatures above 150 K. In our GaN powder, we clearly observe UVL signatures and this deviation from the usual GaN behaviour can be reasonably explained by weak thermalization of holes from the acceptor to valence bands. The two other blue contributions are less common PL bands in bulk GaN. The contribution of the above-mentioned defect-related bands are not clear, but can be tentatively attributed to residual impurities or/and structural disorder observed on the crystallite surfaces. However, it seems to be sensitive to the nature of the crystallites/matrix interface as mentioned below.

The dominating and regular YL band GaN is located approximately in the same position as observed in the PL spectra of GaN quantum wells and dots elaborated with different methods [21–26]. Reynolds et al. [21] have shown that the occurrence of the YL band in the GaN epilayer deposited by MBE is hardly related to the presence of oxygen. This is also suggested by the results of Moon et al. [27]. Due to the low formation energies of the gallium (V_{Ga}) and nitrogen (V_N) vacancies in undoped GaN [28], it is natural to expect that these native defects will be the dominant ones. On the other hand, V_{Ga} could easily diffuse and would form complexes defect most likely with donors such as oxygen in nitrogen sites (O_N), which is a shallow donor with an ionisation energy of 32 meV [29]. V_{Ga} is a triple acceptor completely filled with electrons, and the positively charged O_N attracts each other forming a double acceptor V_{Ga}–O_N or/and other complexes such as V_{Ga}–O_{2N} completely filled with electrons and in equilibrium, i.e. $(V_{Ga}–O_N)^{2-}$ and $(V_{Ga}–O_{2N})^{1-}$. It is also possible that V_{Ga} forms a complex defect with Si_N. However, this is unlikely because the bounding energy of this complex is low compared to that of V_{Ga}–O_N [30]. The most favourable sites to form these complexes are the grain boundaries, dislocations and crystallite surfaces, in agreement with previous works that depicted the presence of negatively charged dislocations [31]. This is also the view of Shalish et al. [25] who expect a large contribution of grain boundary surfaces to the YL. We then attribute the YL in our samples to the electron transition from the conduction band (or shallow donors) to deep acceptor levels. The defects associated with these levels can be V_{Ga}–O_N complex defects and related complexes formed near the nanocrystallites surface or/and dislocations. This kind of defect density is expected to be large due to the large surface/volume ratio of our small particles. The YL broadening is characteristic of carriers' recombination at deep-level defects, due to strong electron–phonon coupling (Huang–Rhys factor of 6.5). The full-width at half-maximum (FWHM) of the YL is evaluated approximately to 430 meV at $T = 0$ K [32], reasonably close to our measured value (390 meV).

The PL spectra of the GaN–SiO_2 composite (Fig. 4), measured with an excitation wavelength of 325 nm, exhibit the YL of GaN with similar characteristics as previously, but a dominant BL band centred at 2.91 eV. Reshchikov et al. [13] have demonstrated that the BL of the undoped GaN is hardly related to surface states and can be enhanced or quenched by appropriate chemical and/or thermal treatments. Generally, the soft method used to embed GaN in a matrix affects only the surfaces of nanocrystallites. Thus, the unexpected intensity change of the BL GaN (between free and SiO_2 embedded GaN nanocrystals) led us to assume that surface defects are most responsible. The large broadening of the BL is a consequence of the large electron–phonon coupling in the deep BL-related defects. The FWHM (W) temperature dependence of the BL band observed by Reshchikov et al. [33] was best fitted by the formula:

$$W(T) = 340\sqrt{\coth\left(\frac{43}{2\,kT}\right)}$$

where the units of kT and $W(T)$ are in meV. According to this formula $W(300) \approx 412$ meV. This value is comparable to our measured value, 390 meV.

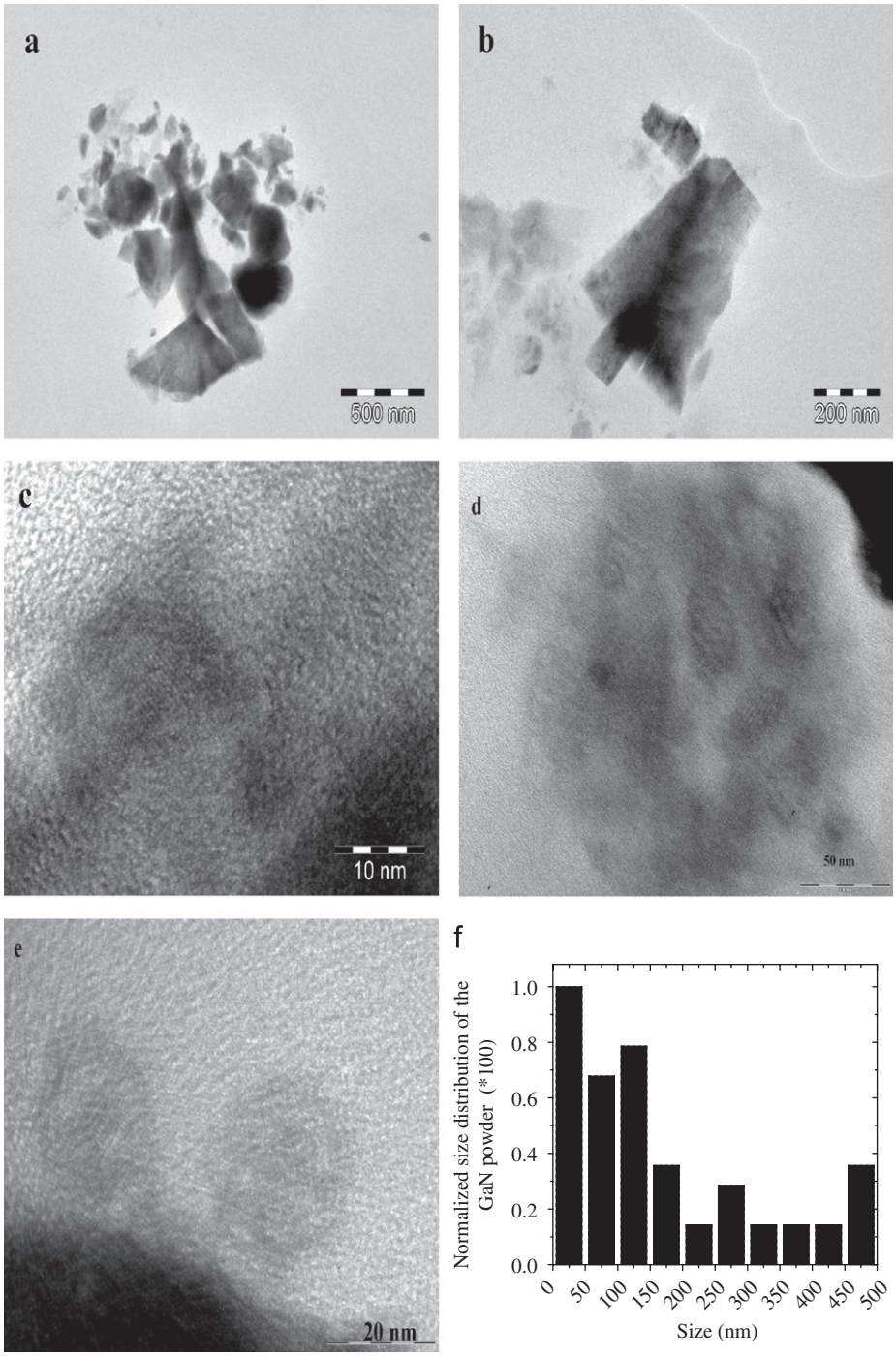

Fig. 2. TEM and HRTEM micrographs of the GaN powder used to dope the SiO_2 matrix. (a) Grains' distributions are multimodal. (b) Larger magnification of an isolated particle showing several subgrains. (c) Large magnification of an isolated grain showing the absence of periodicity at the surface. (d) and (e) show the surface details of some microcrystallites and (f) shows the size distribution of the GaN powder.

The BL is commonly observed in PL and cathodoluminescence (CL) spectra of undoped, Si-doped, Zn-doped or Mg-doped GaN [1,33–35]. The BL studies in the undoped GaN have shown that this band is related to electron transitions from a shallow donor or/and conduction band to a deep acceptor with an energy of about 380 meV above the valence band [33], while the microscopic nature of the acceptor remains uncertain. Recently Reshchikov et al. [34] proposed Zn as the acceptor in undoped GaN. On the contrary, Yang et al. [36] suggested V_{Ga}-related complexes such as V_{Ga}–O_N. Li et al. [12] have established a clear relationship between the BL intensity of unintentionally doped GaN layers and their structural characteristics. In their study the authors have shown that the intensity of BL increases with the χ_{min} of RBS/channelling (Rutherford backscattering) and the FWHM of high-resolution XRD peaks, which means that BL is likely related to intrinsic defects such as dislocations and grain boundaries. Moreover, many spatially resolved CL studies reveal nonuniform distribution of the BL through GaN samples. This is an undeniable proof of the BL-related defects segregation, mainly, around the crystallites surface. Thus, more contribution of the BL in PL spectra of smaller crystallites is expected, since the surface/volume ratio is large in this case. To determine whether the BL is

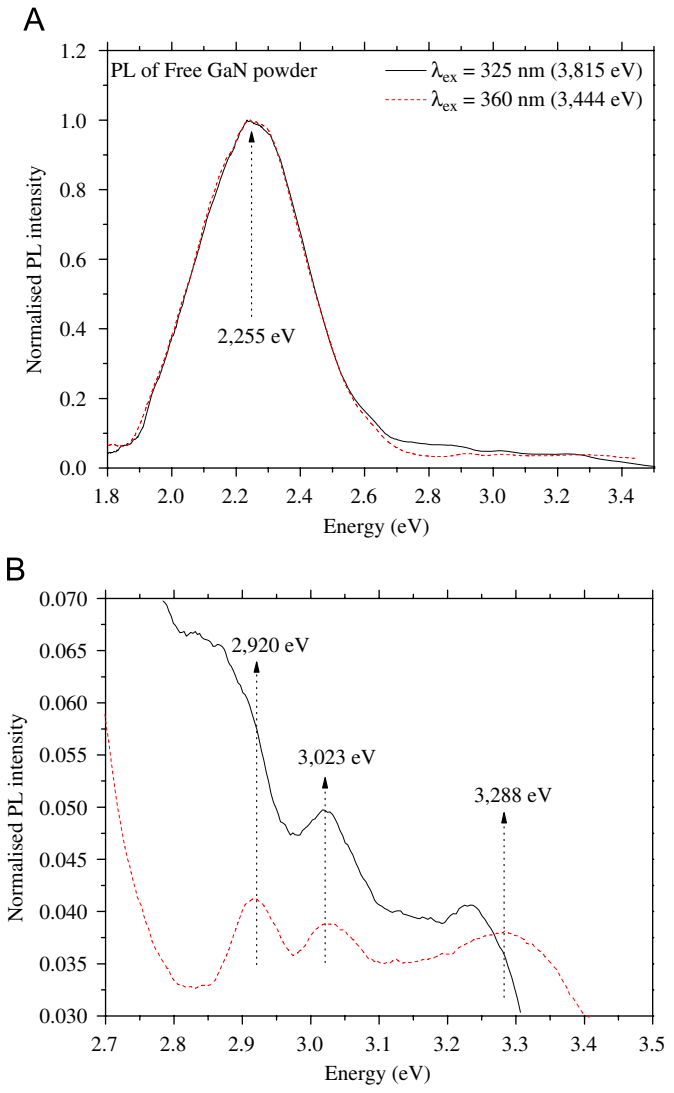

Fig. 3. (A) Room-temperature PL spectrum of the GaN-free powder and (B) spectra details in the energy interval 2.7–3.5 eV.

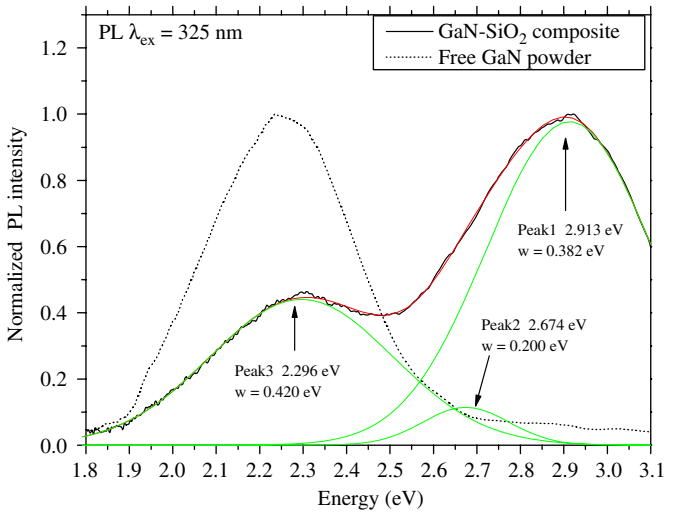

Fig. 4. Room-temperature PL spectrum of the GaN–SiO_2 composite excited with an energy of 3.75 eV (330 nm). Dots are the experiments, while solid lines give the fit with three Gaussian-like bands. The PL spectrum of the GaN-free powder is shown for comparison.

related to surface or bulk defects, other PL measurements were carried out. PL with excitation energy close to the bulk band gap of 360 nm (3.44 eV) was performed in order to excite selectively the biggest crystallites enclosed in our samples. The resulting spectrum (Fig. 5) clearly demonstrates a strong BL decrease in favour of YL. Thus, it is suggested that the smaller nanocrystallites for which surface effects are larger and/or a large absorption at the crystallite surfaces contribute to BL more than the bulk. PL spectrum measured with excitation energy largely above the band gap (Fig. 6) is best fitted with seven emission Gaussian peaks. The prominent one, located at 2.85 eV (peak 4), can be reasonably assigned to defects located at the vicinity of the crystallite's surfaces where the main part of the excitation was absorbed. Peak 2, located at 3.65 eV, corresponds probably to internal transitions in the defects located near the crystallite's surface. Peak 3, located at 3.31 eV, is attributed to near-band-gap luminescence of the GaN crystallites bulk.

The PLE spectra of the GaN–SiO_2 composite and GaN-free powder monitored at the maximum of the YL (~2.25 eV) (Fig. 7)

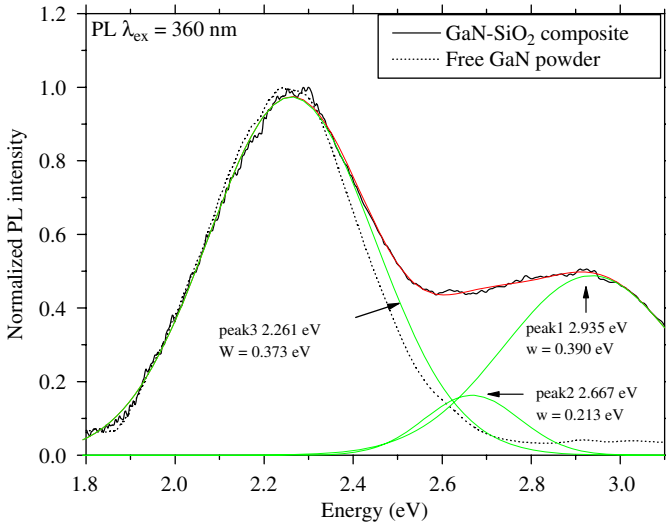

Fig. 5. Room-temperature PL spectrum of the GaN–SiO_2 composite excited with an energy of 3.44 eV (360 nm). Dots are the experiments, while solid lines give the fit with three Gaussian-like bands. The PL spectrum of the GaN-free powder is shown for comparison.

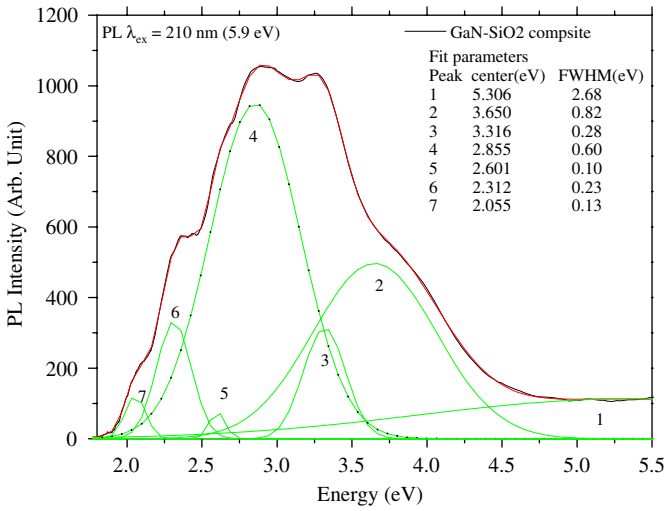

Fig. 6. Room-temperature PL spectrum of the GaN–SiO_2 composite excited with an energy of 5.9 eV (210 nm). Dots are the experiments, and lines give the fit with seven Gaussian-like bands.

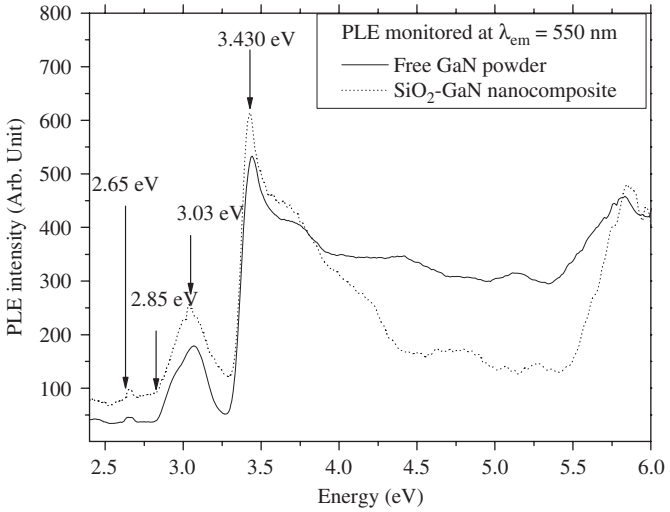

Fig. 7. PLE spectra of YL in the 2.4–6.0 eV range at room temperature for the GaN–SiO_2 composite and a GaN-free powder.

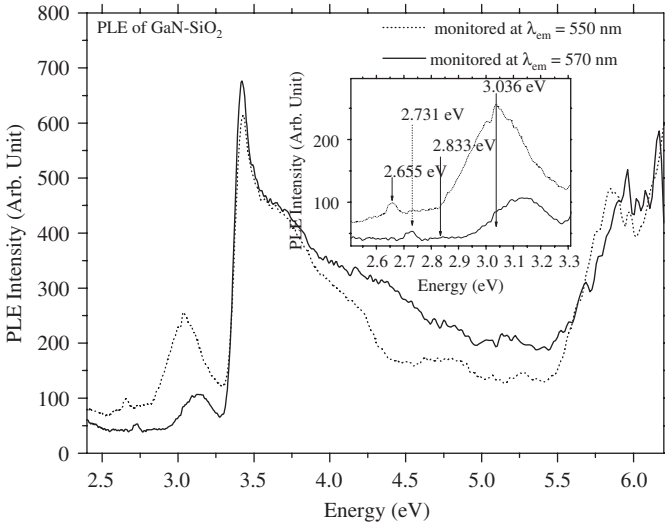

Fig. 8. PLE spectrum of YL in the 2.4–6.5 eV range at room temperature of the GaN–SiO_2 composite. The inset shows the details of the YL resonant part.

exhibit an unusual large signal, compared to a bulk, in the range below the gap. A possible explanation for this behaviour is the large defect density responsible for YL, in agreement with the assignment of the YL to surface defects and/or dislocations. The intense peak at 3.43 eV corresponds to bulk-like (biggest) crystallites band gap. We note also an extended structure signal above the band gap, which can be attributed to the multimodal crystallites sizes. The intensity of this peak is large because the absorption coefficient increases considerably in the near-band-gap range. Thus, a high density of electron–hole pairs is generated near the crystallites surface where they recombine, giving rise to YL. The YL mechanism may be described in the following way: firstly, the photo-generated hole is rapidly trapped in the YL-related defects located near the surface. Secondly, the exited defect recombines with the photo-generated electron, radiating YL.

The weak peak at 2.65 eV in PLE, also appearing in PL measurements (see Figs. 4–6), corresponds to the electron transition from YL-related defects, presumably the deep V_{Ga}–O_N acceptors or/and V_{Ga}–O_{2N}, to the conduction band. In the configuration coordinate (CC) model, this value $E_0 \approx 2.65$ eV represents the zero-phonon energy, below which the excitation of the YL band is impossible (see Ref. [8] and references therein). E_0 was evaluated to 2.64 eV at $T = 0$ K in Ref. [32]. Elsner et al. [37] have calculated, using *ab initio* local DFT, the transition and formation energies of V_{Ga}–O_N and other complexes of the same family at the stress field of the threading-edge dislocations in GaN. They found that the most favourable position for these defects is at the dislocation core with energy transitions, with respect to the valence band maximum, $E^{1-/2-} = 1$ eV and $E^{0/1-} = 0.7$ eV for V_{Ga}–O_N and V_{Ga}–O_{2N}, respectively. Subtracting these values from our observed gap energy (3.43 eV) gives transition energies of 2.43 and 2.73 eV for V_{Ga}–O_N and V_{Ga}–O_{2N}, respectively. According to Elsner et al.'s [37] calculations, the V_{Ga}–O_{2N} and V_{Ga}–O_N defects can be the prevailing ones in our GaN nanocrystallites. Regarding the band centred at 3.03 eV, we think that it can correspond to the nearly vertical transitions in the CC diagram in adiabatic approximation. Usually the resonant part of the YL-PLE spectrum of the GaN bulk crystals is structureless and can be fitted with a Gaussian curve with a maximum at 3.19 eV and an FWHM of 0.4 eV ($T = 4$ K) [32]. The YL band is by far the most studied PL band in GaN; however, it is still not clear how many kinds of defects contribute to that band. PLE measurements monitored at 2.17 eV (Fig. 8), slightly below the centre of the YL

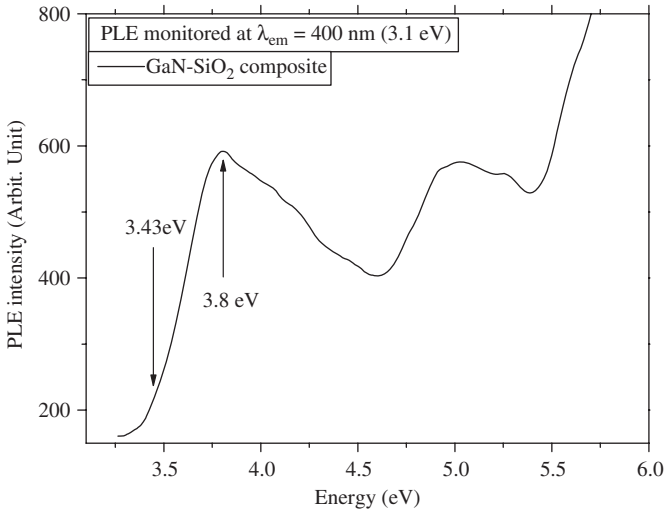

Fig. 9. Room-temperature PLE spectrum of the GaN–SiO_2 composite monitored maximum in the blue region.

band, provide 2.73 eV for ZPL (E_0) and 3.15 eV for the vertical transitions. The observed changes indicate that the YL band is related to several defects with different ZPLs rather than a single defect in agreement with high-energy PL where we observed two separate bands (peaks 7 and 6 in Fig. 6).

The PLE of GaN–SiO_2 nanocomposite (Fig. 9) monitored at the blue region shows that absorption begins with a linear increase to 3.50 eV and reaches its maximum value at 3.8 eV, which may be related to the ionisation of crystallites. This indicates that BL originates from the smallest nanocrystallites or/and from the crystallite surfaces because the absorption is significant in the energy ranges corresponding to the smallest crystallites or/and to chemical species located at the surfaces.

4. Conclusion

GaN-free nanopowder and GaN–SiO_2 nanocompsite were studied with XRD, TEM, PL and PLE techniques. The structural study revealed flattened mean crystallite shapes with sizes evaluated to around 150 nm. On the PL spectra of the GaN-free

powder, we observed strong broad YL band, weak BL and weak UVL. For the composite, in all cases, the PL was dominated by YL and BL centred at ~2.25 and ~2.9 eV, respectively. The PL spectra excited with photon energy close to the band gap are dominated by the YL band, whereas when the excitation energy reaches values above the band gap the BL predominates. We attribute this behaviour to the large contribution of crystallite surfaces to BL. The PLE measurement was used to prospect the deep levels related to the YL. These measurements indicated that the YL is due to a superposition of two types of defects with ionisation energies of 2.65 and 2.73 eV (the energy required to promote the electron from the charged defect to the CB). The most probable defects with regard to the previous criteria are $(V_{Ga}–O_{2N})^{1-}$ and $(V_{Ga}–O_N)^{2-}$ complex defects segregated near the crystallites surface or/and other undetermined extended bulk defects.

References

[1] I.V. Kityk, M. Nyk, W. Strek, J.M. Jablonski, J.M. Misiewicz, J. Phys.: Condens. Matter 17 (2005) 5235.
[2] Todd Steiner (Ed.), Semiconductor Nanostructures for Optoelectronic Applications, Artech House, Inc., Boston, London, 2004.
[3] S.C. Jain, M. Willander, J. Narayan, R.V. Overstraeten, J. Appl. Phys. 87 (3) (2000).
[4] J.W. Orton, C.T. Foxon, Rep. Prog. Phys. 61 (1998) 1.
[5] F.A. Ponce, D.P. Bour, Nature 386 (1997) 351.
[6] Y.S. Park, J. Korean Phys. Soc. 34 (1999) S199.
[7] S. Nakamura, Semicond. Sci. Technol. 14 (1999) R27.
[8] M.A. Reshchikov, H. Morkoç, J. Appl. Phys. 97 (2005) 061301.
[9] F. Widmann, J. Simon, B. Daudin, G. Feuillet, J.L. Rouvière, N.T. Pelekanos, Phys. Rev. B 58 (24) (1998).
[10] S.H. Shim, K.B. Shim, J. Yoon, Y. Shimizu, T. Sasaki, N. Koshizaki, Thin Solid Films 472 (2005) 11.
[11] M. Shimada, Y. Azuma, K. Okuyama, Y. Hayashi, E. Tanabe, Jpn. J. App. Phys. 45 (1A) (2006) 328.
[12] Shuti Li, F. Jiang, G. Han, L. Wang, C. Xiong, X. Peng, H. Mo, Mater. Sci. Eng. B 122 (2005) 72.
[13] M.A. Reshchikov, P. Visconti, H. Morkoç, Appl. Phys. Lett. 78 (2) (2001).
[14] D.J. Duval, B.J. McCoy, S.H. Risbut, Z.A. Munir, Appl. Phys. Lett. 83 (1998) 2301.
[15] M. Morales, D. Chateigner, L. Lutterotti, J. Ricote, Mater. Sci. Forum 408–412 (2002) 113.
[16] Lutterotti, Matthies, Wenk, MAUD (Material Analysis Using Diffraction): a user friendly Java program for Rietveld texture analysis and more, National Research Council of Canada, Ottawa, 1999, pp. 1599–1604.
[17] A. Le Bail, J. Non-Cryst. Solids 183 (1995) 39.
[18] N.C. Popa, The $(h\,k\,l)$ dependence of diffraction-line broadening caused by strain and size for all Laue groups in Rietveld refinement, JAC 31, 1998, pp. 176–180.
[19] Daniel Chateigner, Xiaolong Chen, Marco Ciriotti, Robert T. Downs, Saulius Gražulis, Armel Le Bail, Luca Lutterotti, Yoshitaka Matsushita, Peter Moeck, Miguel Quirós Olozábal, Hareesh Rajan, Alexandre F.T. Yokochi, Crystallography Open Database (COD): 〈www.crystallography.net〉, 2003.
[20] D. Chateigner (Ed.), Combined analysis: structure–texture–microstructure–phase–stresses–reflectivity analysis by X-ray and neutron scattering, 2004, p. 147, 〈http://www.ecole.ensicaen.fr/~chateign/texture/combined.pdf〉.
[21] D.C. Reynolds, D.C. Look, B. Jogai, J.E. Van Nostrand, R. Jones, J. Jenny, Solid State Commun. 106 (10) (1998) 701.
[22] M. Nyk, J.M. Jablonski, W. Strek, J. Misiewicz, Opt. Mater. 26 (2004) 133.
[23] J.A. Wolk, K.M. Yu, E.D. Bourret-Courchesne, Appl. Phys. Lett. 70 (17) (1997).
[24] R. Dawili˜ski, R. Doradzi˜ski, J. Garczy˜ski, L. Sierzputtowski, M. Palczewska, A. Wysmolek, M. Kami˜ska, MRS Internet J. Nitride Semicond. Res. 3 (1998) 25.
[25] I. Shalish, L. Kronik, G. Segal, Y. Rosenwaks, Yoram Shapira, Phys. Rev. B 59 (15) (1999).
[26] I. Shalish, C.E.M. de Oliveira, Yoram Shapira, J. Salzman, Phys. Rev. B 64 (2001) 205313.
[27] Yong-T. Moon, Dong-J. Kim, Jin-S. Park, Jeong-T. Oh, Yoon-S. Kim, Nae-M. Park, Baek-H. Kim, Seong-J. park, J. Cryst. Growth 248 (2003) 494.
[28] S. Limpijumnong, C.G. Van de Walle, Phys. Rev. B 6 (2004) 035207.
[29] H. Wang, A.-B. Chen, J. Appl. Phys. 87 (2000) 7859.
[30] J. Neugebauer, C.G. Van de Walle, Appl. Phys. Lett. 69 (1996) 503.
[31] P.J. Hansen, et al., Appl. Phys. Lett. 72 (1998) 2247.
[32] T. Ogino, M. Aoki, Jpn. J. Appl. Phys. 19 (1980) 2395.
[33] M.A. Reshchikov, F. Shahedipour, R.Y. Korotkov, B.W. Wessels, M.P. Ulmer, J. Appl. Phys. 87 (7) (2000).
[34] M.A. Reshchikov, H. Morkoç, R.J. Molnar, D. Tsvetkov, V. Dmitriev, Mater. Res. Soc. Symp. Proc. 743 (2003).
[35] Y. Koide, D.E. Walker Jr., B.D. White, L.J. Brillson, T. Itoh, R.L. McCreery, M. Murakami, S. Kamiyama, H. Amano, I. Akasaki, Phys. Status Solidi B 240 (2) (2003) 356.
[36] H.C. Yang, T.Y. Lin, Y.F. Chen, Phys. Rev. B 62 (2000) 12593.
[37] J. Elsner, R. Jones, M.I. Heggie, S. Öberg, P.B. Briddon, Phys. Rev. B 58 (19) (1998).